Available online at www.sciencedirect.com
SCIENCE DIRECT®
Journal of Nuclear Materials 355 (2006) 38–46
journal of nuclear materials
www.elsevier.com/locate/jnucmat

The relative impact of radiolysis products in radiation induced oxidative dissolution of UO_2

Ella Ekeroth, Olivia Roth, Mats Jonsson *

KTH Chemical Science and Engineering, Nuclear Chemistry, Royal Institute of Technology, SE – 100 44 Stockholm, Sweden

Received 23 December 2005; accepted 5 April 2006

Abstract

The relative impact of radiolysis products in radiation induced oxidative dissolution of UO_2 has been studied experimentally. The experiments were performed by γ-irradiating an aqueous solution containing HCO_3^- and a UO_2-pellet. The U(VI) concentration in the solution was measured as a function of irradiation time. The aqueous solution was saturated with Ar, N_2O, N_2O/O_2 (80/20), air and O_2 in order to vary the conditions and the initial oxidant yields. The measured rate of oxidation was significantly higher for the O_2- and air saturated systems compared to the other systems. Using oxidant concentrations derived from numerical simulations of the corresponding homogeneous systems and previously determined rate constants for oxidation of UO_2, the relative trend in rate of oxidation in the different systems was reproduced. The results from the simulations were also used to estimate the relative impact of the oxidative radiolysis products as a function of irradiation time, both for γ- and α-irradiated systems. For γ-irradiated systems saturated with Ar, air or O_2, the most important oxidant is H_2O_2 while for N_2O- and N_2O/O_2-saturated systems the most important oxidant is $CO_3^{\bullet-}$. For α-irradiated systems the most important oxidant was found to be H_2O_2.

1. Introduction

The solubility of UO_2 is assumed to limit the release of radio-toxic species from a future deep repository for spent nuclear fuel to the environment [1,2]. Under reducing conditions, i.e. the expected conditions at the depth of a deep repository, the solubility of UO_2 in ground water is very low and the release rate is therefore also expected to be low [3]. Radiation from the spent nuclear fuel in contact with water will cause radiolysis of water producing reactive radical and molecular products. Both oxidants ($OH^{\bullet}$, H_2O_2, $O_2^{\bullet-}$, $HO_2^{\bullet}$ and O_2) and reductants (e_{aq}^-, $H^{\bullet}$ and H_2) are produced upon radiolysis of water [4]. The oxidants produced alter the otherwise reducing conditions, and can thereby cause oxidation and dissolution of the spent nuclear fuel matrix. When carbonate is present, as in Swedish ground water where the concentration is 2–10 mM [5], $OH^{\bullet}$ will quantitatively be converted into $CO_3^{\bullet-}$, this also being a strong oxidant ($E^0 = 1.9$ V and 1.59 V vs. NHE, respectively [6,7]). Carbonate is also known to form strong soluble complexes with UO_2^{2+} [8] and thereby enhance the solubility of U(VI).

* Corresponding author. Tel.: +46 8790 9123; fax: +46 8790 8772.
E-mail address: matsj@nuchem.kth.se (M. Jonsson).

0022-3115/$ - see front matter © 2006 Elsevier B.V. All rights reserved.
doi:10.1016/j.jnucmat.2006.04.001

In previous years, the main focus has been to study the oxidative dissolution by using H_2O_2 and O_2 as oxidants, and to measure the release of U(VI) as a function of time [9–11]. Another approach has been to use spent nuclear fuel [12], externally γ- and α-irradiated [13,14] and α-doped UO_2 [15] and monitor produced H_2O_2, O_2 and H_2 as well as dissolved uranium, fission products and transuranium elements. Although these studies provide detailed information concerning dissolution dynamics and mass balance, they do not provide information concerning the kinetics of elementary reactions. The latter being a prerequisite for accurate simulation of spent nuclear fuel dissolution. The importance of radiolytically produced radicals on UO_2 dissolution has also been discussed to some extent [16]. In a kinetic and mechanistic study on oxidation of UO_2 powder in aqueous suspension, we measured the consumption of oxidant as a function of time and determined the second order rate constants for UO_2 oxidation [17]. On the basis of these results we found a relationship between the logarithm of the rate constant for oxidation of UO_2 and the one-electron reduction potential of the oxidant. This relationship was based on experimental observations including both one- and two-electron oxidants, and we concluded that the rate limiting step is one-electron transfer regardless of the nature of the oxidant. However, the relationship is based on experiments where no carbonate was added. Hence, the observed rate constants and thereby the relationship itself, are influenced by the kinetics for dissolution of U(VI). The dissolution independent rate constant for oxidation of UO_2 (the rate constant determined under conditions where the rate limiting step is oxidation rather than dissolution) has recently been found to be about five times higher (for H_2O_2) [18] than the originally published value. However, the relative trend given by the relationship should still be valid. From this relationship it can be concluded that $OH^{\cdot}$ and $CO_3^{\cdot-}$ are significantly more reactive towards the UO_2-matrix than H_2O_2 and O_2, the former having significantly higher one-electron reduction potentials [6,7]. In fact, oxidation of UO_2 by both $OH^{\cdot}$ and $CO_3^{\cdot-}$ is diffusion controlled. On the basis of reactivity alone, the importance of radical radiolysis products on spent nuclear fuel dissolution can be assumed to be significant. However, the significance of radical radiolysis products on the dissolution of spent nuclear fuel has never been unambiguously proven.

In this work, we have studied the relative impact of radical and molecular radiolysis products on oxidative dissolution of UO_2. This was done by analyzing the amount of dissolved UO_2^{2+} as a function of time in γ-irradiated aqueous carbonate solutions containing a UO_2-pellet. The main reason for using γ-radiolysis was to obtain high radiation chemical yields for radical products. The conditions were varied by saturating the solutions with different gases or gas-mixtures (Ar, N_2O, O_2, air and N_2O/O_2 (80/20 mol%)). These gases or gas mixtures where chosen to promote production of $CO_3^{\cdot-}$ or $O_2^{\cdot-}$ under γ-irradiation. Using numerical simulations (MAKSIMA-CHEMIST [19]) of the homogenous system in combination with the experimental observations we have been able to assign the relative impact of the radiolysis products under various conditions. For comparison, simulations on α-irradiated systems have also been conducted.

2. Experimental

In these studies, a UO_2-pellet (U-235 nominal enrichment = 0.711) was immersed in 10 ml 10 mM $NaHCO_3$-solution. By using carbonate throughout the experiments, the oxidation reaction on the UO_2 surface will not be blocked or delayed by dissolution of the oxidation product. The solution was purged and saturated with (one of) the gases or gas mixtures: Ar, N_2O, O_2, air, N_2O/O_2 (80/20 mol%). The solution containing the pellet was thereafter irradiated in a ^{60}Co-source at room temperature. The dose rate was 0.06 Gy/s (determined using Fricke dosimetry [4]). Samples were taken at different time intervals for analysis of dissolved uranium using a Scintrex UA-3 Uranium Analyzer [20]. The UO_2-pellet was washed with 10 mM carbonate solution three times in order to remove already oxidized U(VI) on the surface prior to each experiment. Reference experiments corresponding to the experimental conditions described above were performed without γ-irradiation and were used for background corrections. Milli-Q filtered water was used throughout. The UO_2-pellet was supplied from Westinghouse Atom AB, gases and chemicals used were from AGA, Merck and Scintrex Limited.

3. Results and discussion

Under the conditions used in our experiments, i.e. 10 mM HCO_3^-, oxidation of UO_2 rather than dissolution of oxidized UO_2 has been shown to be the rate limiting step [18]. Hence, the measured rate of dissolution will be identical to the total rate of

oxidation, this in turn being equal to the sum of the rates of oxidation for all oxidants. This is a prerequisite for comparing the relative impact of the radiolytical oxidants. Furthermore, in the presence of 10 mM HCO_3^-, the initially produced $OH^\cdot$ is quantitatively converted into $CO_3^{\cdot-}$. When saturating the solution with N_2O and N_2O/O_2 the initially produced e_{aq}^- is quantitatively converted into $OH^\cdot$ (reaction (1)) and consequently the initial yield of $CO_3^{\cdot-}$ is increased.

$$e_{aq}^- + N_2O + H_2O \rightarrow OH^\cdot + N_2 + OH^- \quad (1)$$

In the presence of O_2 the initially produced solvated electron, e_{aq}^-, is quantitatively converted into $O_2^{\cdot-}$. However, when using the N_2O/O_2 (80/20) mixture, conversion into $OH^\cdot$ is kinetically favored. The *G*-values (radiation chemical yields) for $CO_3^{\cdot-}$ and $O_2^{\cdot-}$ for the aqueous solutions used in this work are summarized in Table 1.

In Fig. 1, the amount of dissolved U(VI) is shown as a function of irradiation time. The values presented are corrected with respect to background experiments using Ar. It should be noted that the background correction is of marginal importance.

Table 1
G-values for $O_2^{\cdot-}$ and $CO_3^{\cdot-}$ [21]

Gas	$G(O_2^{\cdot-})$ (μmol J^{-1})	$G(CO_3^{\cdot-})$ (μmol J^{-1})
Ar	0	0.28
N_2O	0	0.56
N_2O/O_2	0	0.56
Air	0.28	0.28
O_2	0.28	0.28

Table 2
Rate of oxidative dissolution of UO_2

Gas	Rate (μmol min^{-1})
Ar	$(8 \pm 1) \times 10^{-5}$
N_2O	$(9 \pm 2) \times 10^{-5}$
N_2O/O_2	$(6 \pm 1) \times 10^{-5}$
Air	$(1.5 \pm 0.2) \times 10^{-4}$
O_2	$(3.0 \pm 0.2) \times 10^{-4}$

As can be seen in Fig. 1, the amount of dissolved U(VI) appears to increase linearly with irradiation time in all cases. The slope gives the rate of dissolution and thereby the rate of oxidation. The resulting dissolution rates are summarized in Table 2.

It is obvious that the dissolution rate is significantly higher for the O_2- and air-saturated solutions where production of $O_2^{\cdot-}$ is enhanced. $CO_3^{\cdot-}$ is produced in all systems, however, there is no significant increase in the rate of dissolution when the *G*-value is increased by a factor of 2 (N_2O and N_2O/O_2). It should be noted that the oxidizing capability (reflected by the reduction potential) and thereby the reactivity of $O_2^{\cdot-}$ is estimated to be several orders of magnitude lower than that of $CO_3^{\cdot-}$. Hence, the observed dissolution rates cannot be understood solely in terms of relative reactivity and initial yields of radiolysis products.

To further analyze the reaction conditions we performed numerical simulations using MAKSIMA-CHEMIST. In the simulations the different gases

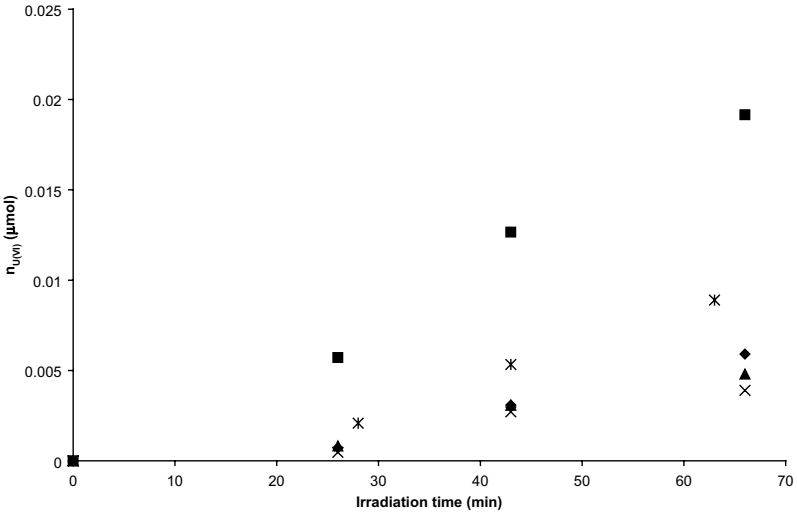

Fig. 1. Amount of dissolved U(VI) as a function of γ-irradiation time (◆ N_2O, ▲ Ar, ■ O_2, × N_2O/O_2, ∗ air).

Table 3
Calculated steady-state and mean concentrations of oxidants

	$[H_2O_2]$ (mol dm^{-3})	$[O_2]$ (mol dm^{-3})	$[O_2^{\cdot-}]$ (mol dm^{-3})	$[HO_2^{\cdot}]$ (mol dm^{-3})	$[CO_3^{\cdot-}]$ (mol dm^{-3})	$[OH^{\cdot}]$ (mol dm^{-3})
Ar	1.28×10^{-6}	4.55×10^{-6}	2.88×10^{-8}	4.23×10^{-10}	3.00×10^{-9}	1.93×10^{-13}
N_2O	1.08×10^{-6}	3.70×10^{-5}	2.10×10^{-9}	3.57×10^{-10}	3.66×10^{-8}	3.27×10^{-13}
N_2O/O_2	1.08×10^{-6}	3.00×10^{-4}	2.20×10^{-9}	3.57×10^{-10}	3.55×10^{-8}	3.23×10^{-13}
Air	1.70×10^{-5}	2.47×10^{-4}	4.00×10^{-7}	5.60×10^{-9}	2.35×10^{-10}	1.70×10^{-13}
O_2	2.20×10^{-5}	1.37×10^{-3}	4.70×10^{-7}	7.40×10^{-9}	1.75×10^{-10}	1.63×10^{-13}
H_2	6.50×10^{-9}	2.34×10^{-14}	8.82×10^{-12}	2.16×10^{-12}	2.82×10^{-10}	2.59×10^{-14}

and gas mixtures were accounted for but reactions with the UO_2-surface were not included, the systems were treated as being homogeneous. The homogenous reaction rate constants for radiolysis of water were obtained from NDRL/NIST Solution Kinetics Database [22]. Steady-state concentrations were reached within a relatively short time for most radicals while the concentrations of the molecular products were increasing and never reached steady-state within the time used for the simulation and for the experiment. The resulting steady-state concentrations for radicals and average concentrations for molecular products are summarized in Table 3. For comparison, a system saturated with H_2 (40 bar) was also included in the series of simulations.

As can be seen the average concentration of H_2O_2 is significantly higher for the O_2- and air-saturated systems and roughly appears to reflect the relative reactivity. Hence, the observed difference in dissolution rate can, at least qualitatively, be attributed to the difference in H_2O_2 concentration. Indeed, the steady-state concentration of $O_2^{\cdot-}$ is also significantly higher in these two systems. However, since the reactivity of $O_2^{\cdot-}$ is expected to be significantly lower than that of H_2O_2 (based on the reduction potentials [6]) and $[O_2^{\cdot-}] \ll [H_2O_2]$, the observed difference in dissolution rate cannot be directly attributed to the difference in $O_2^{\cdot-}$ concentration. The increased concentrations of H_2O_2 are connected to the increased concentrations of $O_2^{\cdot-}$, the latter being a precursor for H_2O_2. In previous studies, increased corrosion potentials measured in γ-irradiated systems where $O_2^{\cdot-}$ production is favored have been attributed to $O_2^{\cdot-}$ rather than to H_2O_2. On the basis of these observations it has also been concluded that the rate of dissolution is increased due to higher concentrations of $O_2^{\cdot-}$ [16]. Given the relative concentrations and reduction potentials of H_2O_2 and $O_2^{\cdot-}$ and the fact that corrosion potentials depend on concentrations as well as reduction potentials of solutes, this conclusion is indeed surprising. Judging from the data presented in Table 3, corrosion potentials should mainly be attributed to H_2O_2 and O_2.

Table 4
Rate constants for oxidation of UO_2[a]

Oxidant	k (m min^{-1})
H_2O_2	3.52×10^{-6}[b]
O_2	2.33×10^{-8}
$CO_3^{\cdot-}$	1.00×10^{-3}
$OH^{\cdot}$	1.00×10^{-3}
$O_2^{\cdot-}$	1.36×10^{-7}
$HO_2^{\cdot}$	4.53×10^{-4}

[a] The rate constants are based on a relationship between the rate constant for oxidation of UO_2 and the one-electron reduction potential of the oxidant presented in Ref. [6] and the effect of HCO_3^- presented in Ref. [18].

[b] It has been shown that only 80% of the consumed H_2O_2 results in oxidation of UO_2 [23]. The rate constant for oxidation is therefore 80% of the rate constant for consumption of H_2O_2.

To quantitatively analyze the systems we simply use the average or steady-state concentrations of oxidants and the rate constants (determined from the relationship between reduction potential and rate constant) for oxidation of UO_2. The rate constants used here are given in Table 4.

The total rate of dissolution (oxidation) is given by Eq. (2):

$$\text{rate} = \frac{dn_{U(VI)}}{dt} = A_{UO_2} \sum_{ox=1}^{n} k_{ox}[ox]\frac{n_{e^-}}{2} \tag{2}$$

A_{UO_2} is the BET surface area of the pellet (estimated from the geometrical surface area, 3.66 cm^2, multiplied by three [24]) and n_{e^-} is the number of electrons involved in the redox process (2 for H_2O_2 and O_2 and 1 for the radicals). The reason for using the BET surface area rather than the geometrical surface area is that the rate constants for UO_2 oxidation, k_{ox}, are based on the BET surface area. Admittedly, n_{e^-} for O_2 should be 4 to account for the full oxidant capacity. However, from a kinetic point of view, the oxidation at each site is a two electron process producing U(VI) and H_2O_2. Using

$n_{e^-} = 4$ would therefore result in an overestimation of the total rate of oxidation. For the γ-irradiated system purged with O_2, $n_{e^-} = 4$ gives 30% higher total rate of oxidation than $n_{e^-} = 2$. The H_2O_2 production from the reaction between O_2 and UO_2 is not accounted for in our model which results in a slight underestimation of the total rate of oxidation. The resulting rates of dissolution (oxidation) for each oxidant and for each system are given in Table 5.

In Fig. 2, the calculated rates of oxidation/dissolution are plotted against the experimentally determined rates.

As can be seen, the correlation between the calculated and the experimentally determined dissolution rates is fairly good. In all cases we underestimate the oxidation/dissolution rates, however, the relative trend is reproduced. The reason for the underestimation will be discussed later.

Given the correlation between the calculated and the experimentally determined dissolution rates we can use the data presented in Table 5 to assign the relative impact of the different radiolysis products in the systems studied here. From the table it is obvious that H_2O_2 has the highest impact on the Ar-, air- and O_2-saturated systems. For the N_2O- and N_2O/O_2-saturated systems, $CO_3^{\bullet-}$ has the highest impact. $CO_3^{\bullet-}$ is also of significant importance in the Ar-saturated system. O_2 has significance in all the systems studied experimentally. Not surprisingly, the relative impact as well as the absolute rate of oxidation by $CO_3^{\bullet-}$ is highest in the two systems where the *G*-value for $CO_3^{\bullet-}$ is highest.

Interestingly, the simulation performed on the H_2-saturated system indicates that the most important oxidant is $CO_3^{\bullet-}$. The total rate of dissolution is significantly lower than for the other systems, the main reason for this being that the O_2 and H_2O_2 concentrations are suppressed by the presence of H_2.

The experimental (and simulated) irradiation time is very short in view of spent fuel dissolution in a deep repository. Furthermore, the relative impact of the different oxidants is time dependent. For these reasons we have performed simulations on the γ-irradiated systems for somewhat longer times. In Figs. 3a–3c, the resulting rates of oxidation by the oxidants of highest impact as well as the total rates of oxidation are plotted as a function of irradiation time for Ar-, N_2O- and O_2-saturated systems.

These plots clearly show that the relative impact of molecular oxidants increases with time in all

Table 5
Calculated rates of oxidation and relative impact of oxidants

	H_2O_2 (μmol min^{-1})	O_2 (μmol min^{-1})	$O_2^{\bullet-}$ (μmol min^{-1})	$HO_2^{\bullet}$ (μmol min^{-1})	$CO_3^{\bullet-}$ (μmol min^{-1})	$OH^{\bullet}$ (μmol min^{-1})	Total (μmol min^{-1})
Ar	4.93×10^{-6} (72.7%)	1.16×10^{-7} (1.7%)	2.15×10^{-9} (0%)	1.05×10^{-7} (1.2%)	1.65×10^{-6} (24.3%)	1.06×10^{-10} (0%)	6.78×10^{-6}
N_2O	4.17×10^{-6} (16.5%)	9.47×10^{-7} (3.7%)	1.57×10^{-10} (0%)	8.87×10^{-8} (0.4%)	2.01×10^{-5} (79.5%)	1.80×10^{-10} (0%)	2.53×10^{-5}
N_2O/O_2	4.16×10^{-6} (13.2%)	7.68×10^{-6} (24.5%)	1.64×10^{-10} (0%)	8.87×10^{-8} (0.3%)	1.95×10^{-5} (62.1%)	1.77×10^{-10} (0%)	3.14×10^{-5}
Air	6.57×10^{-5} (89.6%)	6.32×10^{-6} (8.6%)	2.38×10^{-8} (0%)	1.39×10^{-6} (1.5%)	1.29×10^{-7} (0.2%)	9.33×10^{-11} (0%)	7.33×10^{-5}
O_2	8.50×10^{-5} (69.9%)	3.50×10^{-5} (28.8%)	3.50×10^{-8} (0%)	1.84×10^{-6} (1.2%)	9.61×10^{-8} (0.1%)	8.95×10^{-11} (0%)	1.22×10^{-4}
H_2	2.51×10^{-8} (13.9%)	5.99×10^{-16} (0%)	6.57×10^{-13} (0%)	5.36×10^{-10} (0.3%)	1.55×10^{-7} (85.8%)	1.42×10^{-11} (0%)	1.80×10^{-7}

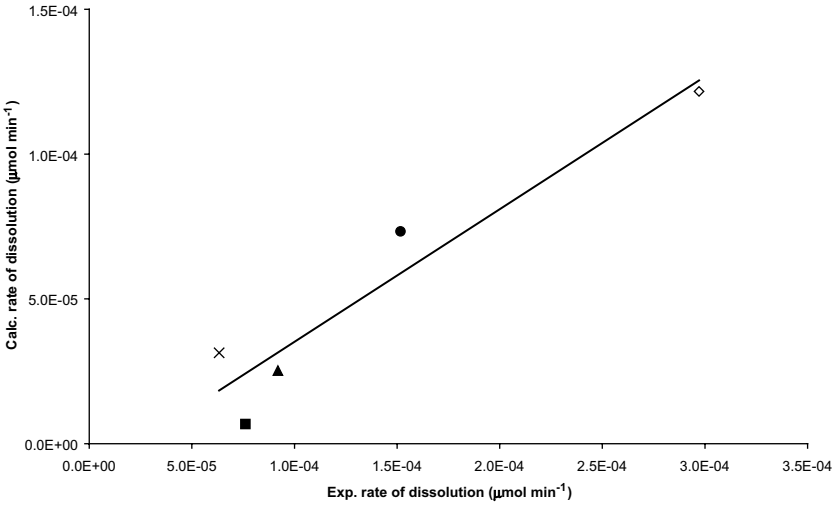

Fig. 2. Calculated rates of oxidation in γ-irradiated systems plotted against the corresponding experimental rates of U(VI)-dissolution (▲ N_2O, ■ Ar, ◇ O_2, × N_2O/O_2, ● air).

three cases. Within less than 100 min, oxidation of UO_2 is completely dominated by molecular oxidants in the Ar-saturated system. For the N_2O-saturated system the relative impact of radical oxidants decreases from 90% to less than 50% in 10 h. Consequently, for time intervals of relevance for dissolution of spent nuclear fuel, oxidation of UO_2 will be governed by molecular oxidants also in a γ-irradiated system.

As can be seen for all three systems, the total rate of UO_2 oxidation/dissolution is increasing with irradiation time and there is no indication that the rate is a approaching a maximum value. However, in a system containing UO_2, the rate of oxidation will approach a maximum value at a steady-state concentration of the oxidants. As mentioned before, reactions with UO_2 are not accounted for in the simulations performed here.

The underestimation of the total rates of oxidation in the experiments described above can also be understood from Figs. 3a–3c. When performing the experiments, the irradiation is interrupted several times since the solution is removed from the γ-source for sampling. After taking the sample,

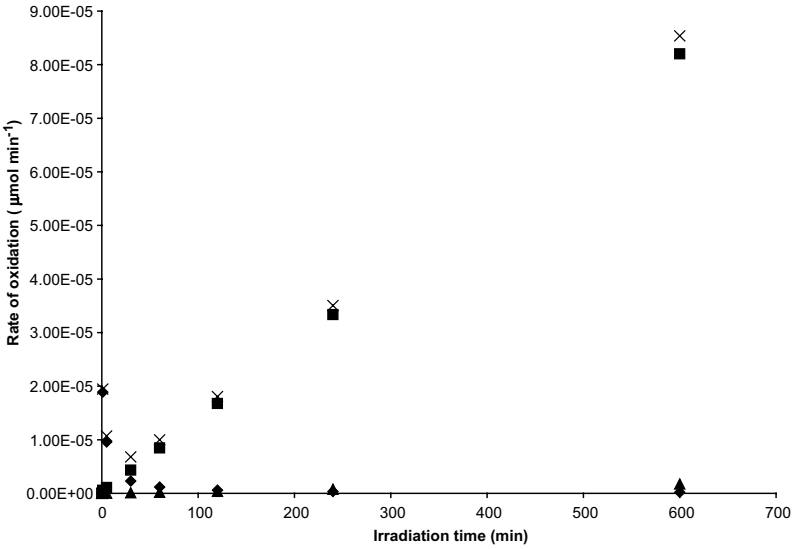

Fig. 3a. Calculated rates of UO_2-oxidation for radiolytically produced oxidants as a function of irradiation time in Ar-saturated aqueous solution (◇ CO_3^{-}, ▲ O_2, ■ H_2O_2, × Tot).

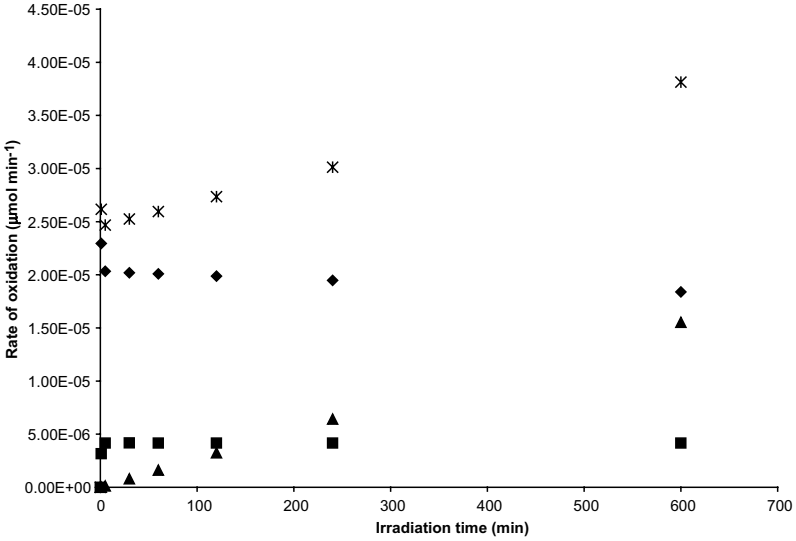

Fig. 3b. Calculated rates of UO_2-oxidation for radiolytically produced oxidants as a function of irradiation time in N_2O-saturated aqueous solution (◆ $CO_3^{\bullet-}$, ▲ O_2, ■ H_2O_2, × Tot).

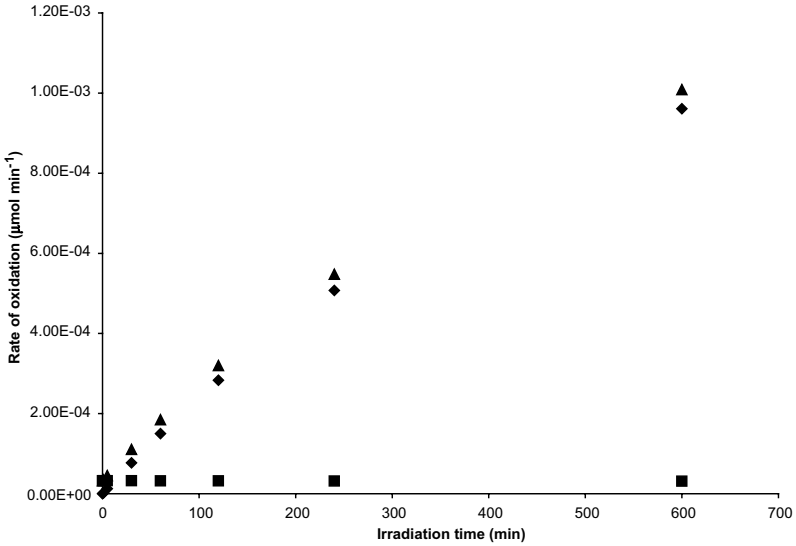

Fig. 3c. Calculated rates of UO_2-oxidation for radiolytically produced oxidants as a function of irradiation time in O_2-saturated aqueous solution (■ O_2, ♦ H_2O_2, ◇ Tot).

the solution is again placed in the γ-source for irradiation. Hence, the total reaction time, including the sampling time, is somewhat longer than the irradiation time, allowing the molecular products longer time for reaction. This is of particular significance for the air- and O_2-saturated systems where the concentrations of H_2O_2 and O_2 are fairly high. The total rate of oxidation for the Ar-saturated system is underestimated by more than one order of magnitude. As can be seen in Fig. 3a, the total rate of oxidation is decreasing with time for the first 30 min. By repeatedly starting the irradiation after each sampling, the actual total oxidation rate will be higher than reflected by the simulation.

In the experiments performed in this work the UO_2 surface exposed to the aqueous solution is relatively small and, consequently, the amount of dissolved U(VI) is also relatively small. The experiments are therefore sensitive to uncertainties in the analysis of the U(VI) concentration. In previous

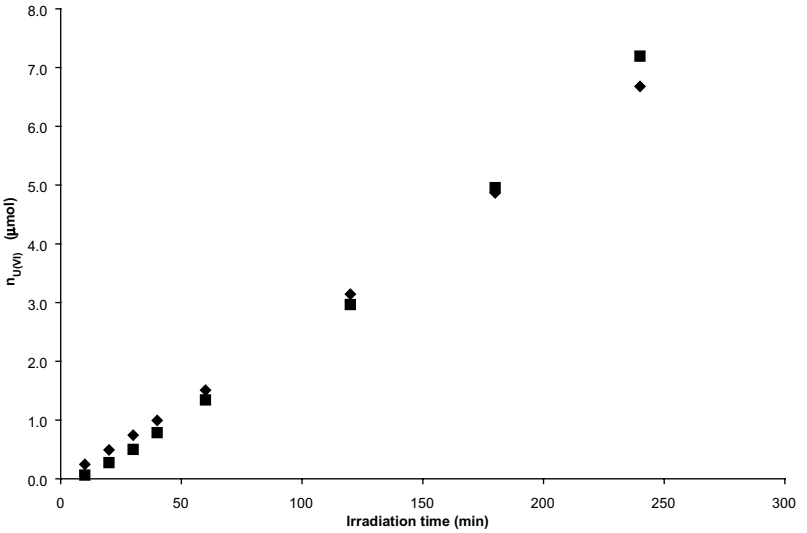

Fig. 4. Estimated (◆) and experimentally determined (■) amount of U(VI) in solution as a function of irradiation time in γ-irradiated UO_2-powder suspensions containing HCO_3^-.

Table 6
Calculated rates of oxidation for α-radiolysis

Conditions	H_2O_2 (µmol min^{-1})	O_2 (µmol min^{-1})	$O_2^{\cdot-}$ (µmol min^{-1})	$HO_2^{\cdot}$ (µmol min^{-1})	$CO_3^{\cdot-}$ (µmol min^{-1})	$OH^{\cdot}$ (µmol min^{-1})	Total (µmol min^{-1})
	4.96×10^{-4}	5.13×10^{-8}	5.24×10^{-9}	1.54×10^{-7}	0	1.65×10^{-10}	4.96×10^{-4}
H_2 (40 bar)	2.01×10^{-6}	2.79×10^{-16}	2.29×10^{-11}	4.81×10^{-10}	0	6.82×10^{-10}	2.01×10^{-6}
H_2 (40 bar) HCO_3^- (10 mM)	1.34×10^{-4}	2.18×10^{-10}	2.57×10^{-9}	2.57×10^{-9}	2.20×10^{-8}	4.84×10^{-12}	1.34×10^{-4}
HCO_3^- (10 mM)	4.69×10^{-4}	4.28×10^{-7}	2.24×10^{-8}	2.24×10^{-8}	1.10×10^{-8}	9.08×10^{-12}	4.69×10^{-4}

studies, we have studied the amount of dissolved U(VI) as a function of irradiation time using N_2O-saturated aqueous UO_2-powder suspensions containing HCO_3^- [23]. In this case the UO_2 surface exposed to the aqueous solution is significantly larger and the amount of dissolved U(VI) is significantly higher. Using the approach elaborated above we have analyzed the previously published results. The experimental results are presented in Fig. 4 along with the corresponding calculated amounts of dissolved U(VI).

As can be seen, the calculated amounts of dissolved U(VI) are virtually identical to the experimental values. Hence, the relatively simple approach used for calculating the rate of UO_2 oxidation/dissolution appears to be very useful. This also shows that the underestimation of the total rate of oxidation resulting from not taking the production of H_2O_2 from the reaction between O_2 and UO_2 into account, is insignificant.

In a deep repository, the radiation chemistry in the vicinity of the fuel surface will be dominated by α-radiolysis. Therefore, we have performed the same type of simulation on α-irradiated systems using the same dose rate. The results (based on a simulated irradiation time of 6 h) are given in Table 6.

An interesting observation here is that the rate of oxidation is completely dominated by H_2O_2 in all four cases (99.9–100%). $CO_3^{\cdot-}$ is of comparable importance only during the first minute of irradiation. The presence of HCO_3^- in the absence of H_2 does not affect the total rate of oxidation significantly. Taking the kinetics for dissolution of oxidized UO_2 into account the presence of HCO_3^- will however have a significant effect. It is also obvious that the presence of H_2 (corresponding to 40 bar pressure) in the absence of HCO_3^- reduces the total rate of oxidation by a factor of 200. In the presence of HCO_3^-, the total rate of oxidation is only reduced by a factor of 3.5 when H_2 is present.

4. Conclusions

In this work we have shown that relatively simple simulations of radiolysis in homogeneous systems can be used to estimate the rate of UO_2 dissolution in systems exposed to γ-radiation. The estimations qualitatively reflect the differences in dissolution rates between different systems (solutions saturated with Ar, N_2O, N_2O/O_2, air or O_2) where a UO_2 pellet in HCO_3^- containing aqueous solution is γ-irradiated. For UO_2-powder suspensions the estimated results are virtually identical to the experimental results. The simulations can also be used to evaluate the relative impact of different oxidants. For systems saturated with Ar, air or O_2, the most important oxidant is H_2O_2 while for N_2O- and N_2O/O_2-saturated systems the most important oxidant is $CO_3^{\bullet-}$. However, the importance of O_2 is increasing with irradiation time in the latter case and for irradiation time longer than 10 h, O_2 will be the most important oxidant in the systems.

Similar simulations were also performed on α-irradiated systems. In these systems the most important oxidant was found to be H_2O_2, also in systems containing H_2 (corresponding to 40 bar).

In conclusion, in systems of relevance for the safety analysis of a deep repository for spent nuclear fuel, only the molecular oxidants are of importance for the dissolution of the fuel matrix.

Acknowledgement

SKB is gratefully acknowledged for financial support.

References

[1] L.H. Johnson, D.W. Shoesmith, Spent Fuel, in: W. Lutze, R.C. Ewing (Eds.), Radioactive Waste Forms for the Future, Elsevier, Amsterdam, 1988, p. 635.
[2] D.W. Shoesmith, J. Nucl. Mater. 282 (2000) 1.
[3] R.L. Segall, R.S.C. Smart, P.S. Turner, Oxide surfaces in solution, in: J. Nowotny, L.-C. Dufour (Eds.), Surface and Near-Surface Chemistry of Oxide Materials, Elsevier Science Publishers B.V., Amsterdam, 1988, p. 527.
[4] J.W.T. Spinks, R.J. Woods, An Introduction to Radiation Chemistry, 3rd Ed., John Wiley & Sons, Inc., New York, 1990.
[5] J.A. T Smellie, M. Laaksoharju, P. Wikberg, J. Hydrol. 172 (1995) 147.
[6] P. Wardman, J. Phys. Chem. Ref. Data 18 (1989) 1637.
[7] R.E. Huie, C.L. Clifton, P. Neta, Radiat. Phys. Chem. 38 (1991) 477.
[8] I. Grenthe, F. Diego, F. Salvatore, G. Riccio, J. Chem. Soc., Dalton Trans. 11 (1984) 2439.
[9] J. Giménez, E. Baraj, M.E. Torrero, I. Casas, J. de Pablo, J. Nucl. Mater. 238 (1996) 64.
[10] J. de Pablo, I. Casas, J. Giménez, M. Molera, M. Rovira, L. Duro, J. Bruno, Geochim. Cosmochim. Acta 63 (1999) 3097.
[11] S.M. Peper, L.F. Brodnax, S.E. Field, R.A. Zehnder, S.N. Valdez, W.H. Runde, Ind. Eng. Chem. Res. 43 (2004) 8188.
[12] T.E. Eriksen, U.-B. Eklund, L. Werme, J. Bruno, J. Nucl. Mater. 227 (1995) 76.
[13] C. Jégou, B. Muzeau, V. Broudic, S. Peuget, A. Poulesquen, D. Roudil, C. Corbel, J. Nucl. Mater. 341 (2005) 62.
[14] S. Sunder, D.W. Shoesmith, N.H. Miller, J. Nucl. Mater. 244 (1997) 66.
[15] C. Jégou, B. Muzeau, V. Broudic, A. Poulesquen, D. Roudil, F. Jorion, C. Corbel, Radiochim. Acta 93 (2005) 35.
[16] H. Christensen, S. Sunder, Nucl. Technol. 131 (2000) 102.
[17] E. Ekeroth, M. Jonsson, J. Nucl. Mater. 322 (2003) 242.
[18] M.M. Hossain, E. Ekeroth, M. Jonsson, J. Nucl. Mater., submitted for publication.
[19] M.B. Carver, D.V. Hanley, K.R. Chaplin, MAKSIMA-CHEMIST a program for mass action kinetics simulation by automatic chemical equation manipulation and integration using stiff techniques, Atomic Energy of Canada Limited – Chalk River Nuclear Laboratories, Ontario, 1979.
[20] J.C. Robbins, CIM Bull. 71 (1978) 61.
[21] G. Choppin, J.O. Liljenzin, J. Rydberg, Radiochemistry and Nuclear Chemistry, Reed Educational and Professional Publishing Ltd., Oxford, 1995.
[22] A.B. Ross, B.H.J. Bielski, G.V. Buxton, D.E. Cabelli, C.L. Greenstock, W.P. Helman, R.E. Huie, J. Grodkowski, P. Neta, NDRL/NIST Solution Kinetics Database, 1992.
[23] M. Jonsson, E. Ekeroth, O. Roth, Mater. Res. Soc. Symp. Proc. 807 (2004) 77.
[24] I. Casas, J. Giménez, V. Marti, M.E. Torrero, J. de Pablo, Mater. Res. Soc. Symp. Proc. 294 (1993) 61.